Cell Reports

Supplemental Information

Formation of the Cortical Subventricular Zone Requires MDGA1-mediated Aggregation of Basal Progenitors

Perez-Garcia and O'Leary

1) SUPPLEMENTAL FIGURES

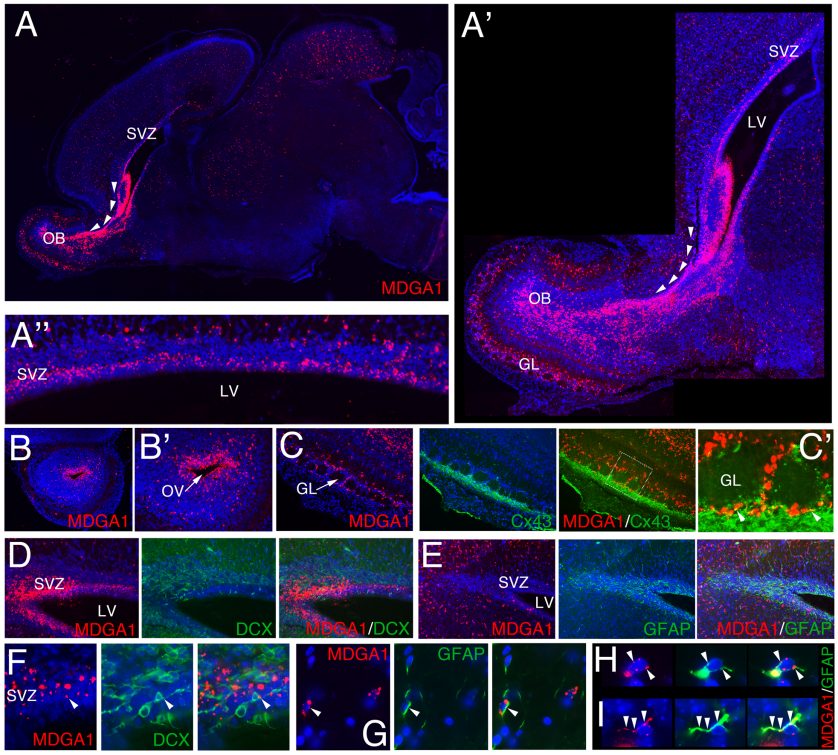

Figure S1. MDGA1 expression in the forebrain, related to Figure 1. Sagittal and coronal sections immunolabeled for MDGA1 (red). DAPI is shown as counterstaining. Merge sections are also shown. A-A": MDGA1 is strongly expressed in the rostral migratory stream (RMS), olfactory bulb (OB) and neocortical SVZ. A'-A'' are high power views of A. Arrowheads in A-A' indicate the RMS. B-C': MDGA1 expression within the OB. MDGA1 is strongly expressed in the proliferative layer surrounding the olfactory ventricle (OV, B-B') and in the glomerular layer (GL) where co-localized with the gap junction protein Connexin43 (Cx43, arrowheads, C-C'). C' is a high power view of C. D-E: Expression of MDGA1 (red) and either Doublecortin (DCX, green in D) or Glial Fibrillary Acidic Protein (GFAP, green in E) in the edge of the cortical RMS. F is a high power view of D. G-I are high power views of E. Arrowheads in F-I indicate co-

localization between MDGA1 and either DCX (F) or GFAP (G-I). Abbreviations: LV: lateral ventricle; SVZ: subventricular zone.

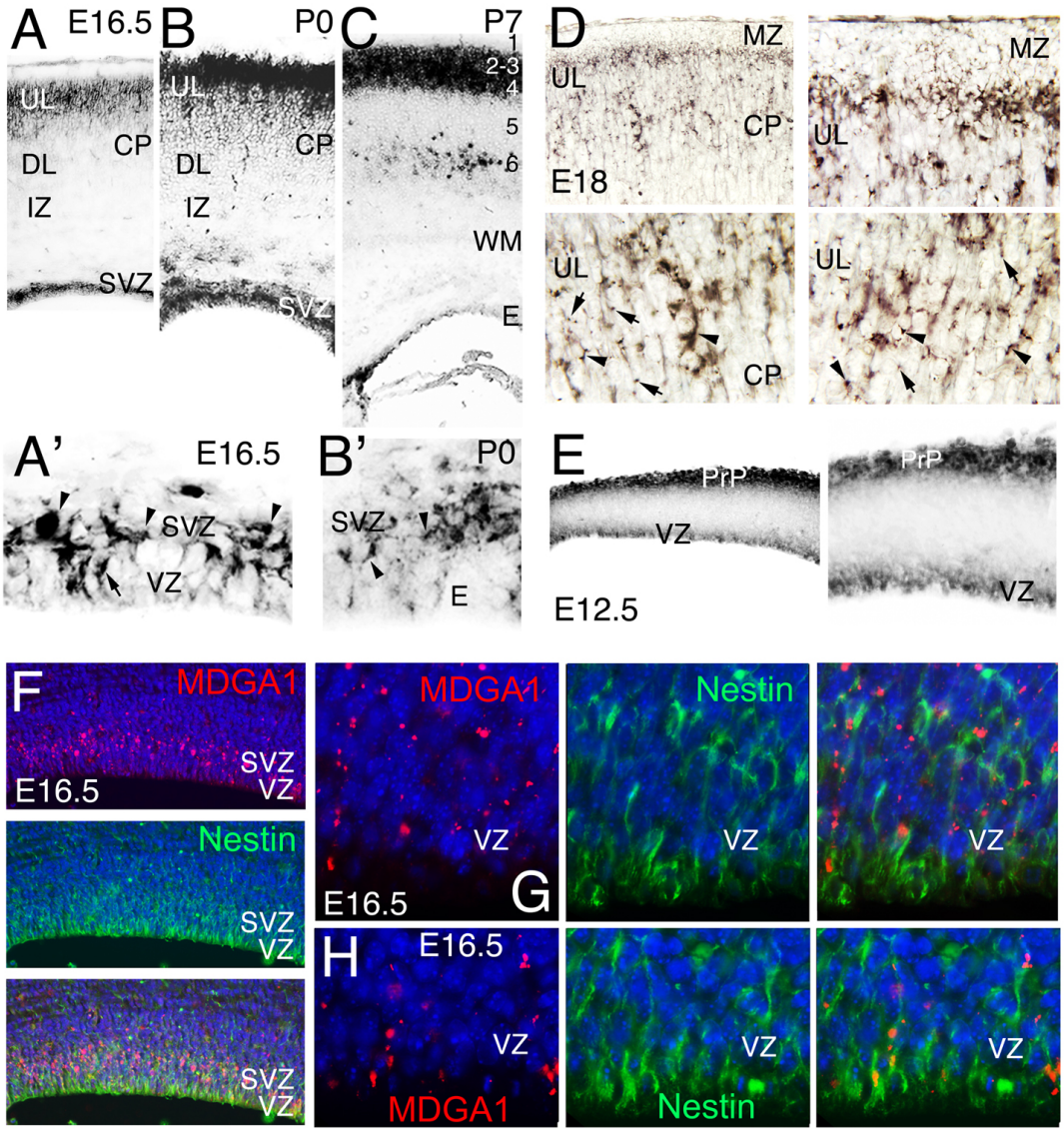

Figure S2. MDGA1 is expressed in the SVZ and in upper layer neurons, related to Figures 1-2. A-C: MDGA1 ISH from E16.5 (A-A'), P0 (B-B') and P7 (C) cortex. A' and B' are high power views at E16.5 and P0, respectively. A-A': At E16.5, MDGA1 is robustly expressed in the subventricular zone (SVZ), with very few expressing cells in the ventricular zone (VZ). MDGA1 is also expressed in upper layer (UL) neurons generated by the SVZ. B-B': At P0, MDGA1 remains highly expressed in the SVZ and upper layers of the cortical plate (CP). C: At P7, MDGA1 expression is limited to the SVZ persisting

at the septo-callosal region. MDGA1 is strongly expressed in the upper layers (layers 2-3 and 4). At the location shown, which is from the primary somatosensory area (S1) of the neocortex, MDGA1 is also expressed in scattered cells in layer 6, which is unique to S1. Arrowheads and arrow in A' and B' point to MDGA1 expressing cells in the SVZ and VZ, respectively. D: At E18, MDGA1 is observed at appositions between migrating upper layer cortical neurons. Arrows and arrowheads indicate small and larger cell-cell contacts between two apposing cells in the upper layers, respectively. E: MDGA1 ISH showing the earliest time-point (E12.5) where MDGA1 transcripts are observed in the cortical VZ, before the SVZ emerges. F-H: Immunolabeling of MDGA1 (red) and Nestin (green) at E16.5 in cortical sections. G-H are high power views of the VZ. DAPI is shown as counterstaining. Merge sections are also shown. MDGA1 is strongly expressed in the cortical SVZ with some expression in the VZ. Nestin is strongly expressed in the VZ and in fibers in the SVZ. MDGA1 immunoreactivity is associated with Nestin positive cells and fibers within the VZ and SVZ. Abbreviations: 1-6: cortical layers 1-6; DL: deeper layers; E: ependyma; IZ: intermediate zone; MZ: marginal zone; PrP: preplate; WM: white matter.

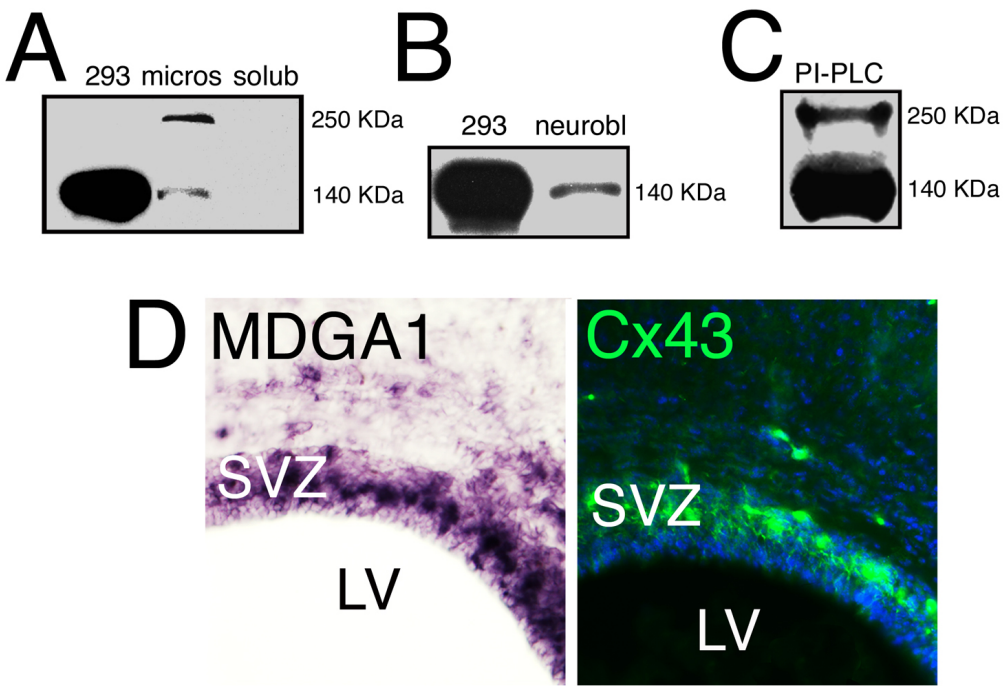

Figure S3. MDGA1 is a plasma membrane protein and interacts with Connexin43, related to Figures 1-3. A-C: Shown is biochemical confirmation that MDGA1 is anchored to the cell membrane by a GPI linkage, for both endogenous MDGA1 in cortex and MDGA1 transfected in 293 cells. A: Differential centrifugation assay performed using tissue from P7 WT cortex. In the immunoblot, MDGA1 protein is present in the microsomal fraction (micros) at the expected size of 140 KDa. MDGA1 is not detected in the soluble fraction (solub). B: Immunoblot showing MDGA1 expressed endogenously in mouse neuroblastoma (neurobl) cell lines at the expected size of 140 KDa. In both immunoblots (A-B), protein extracts of 293 cells transfected with full length MDGA1 are used as a positive controls (293). C: Protein extracts of adult mouse cortex treated with PI-PLC to cleave the GPI linkage that anchors MDGA1 to the cell membrane. In the immunoblot, MDGA1 is detected at the expected size of 140 KDa showing that the PI-PLC treatment releases MDGA1 from the cell membrane and into

the soluble fraction. The immunoblot also detected a band of 250 KDa, suggesting a dimer of MDGA1. D: Co-localization of MDGA1 with Connexin43 (Cx43) in vivo in basal progenitors of the subventricular zone (SVZ) at P0 by using ISH to localize MDGA1 transcripts (purple reaction product) and immunostaining to localize Cx43 (green fluorescence). Both MDGA1 and Cx43 have a robust preferential expression in the SVZ. Abbreviations: LV: lateral ventricle; PI-PLC: phosphatidylinositol-specific phospholipase C.

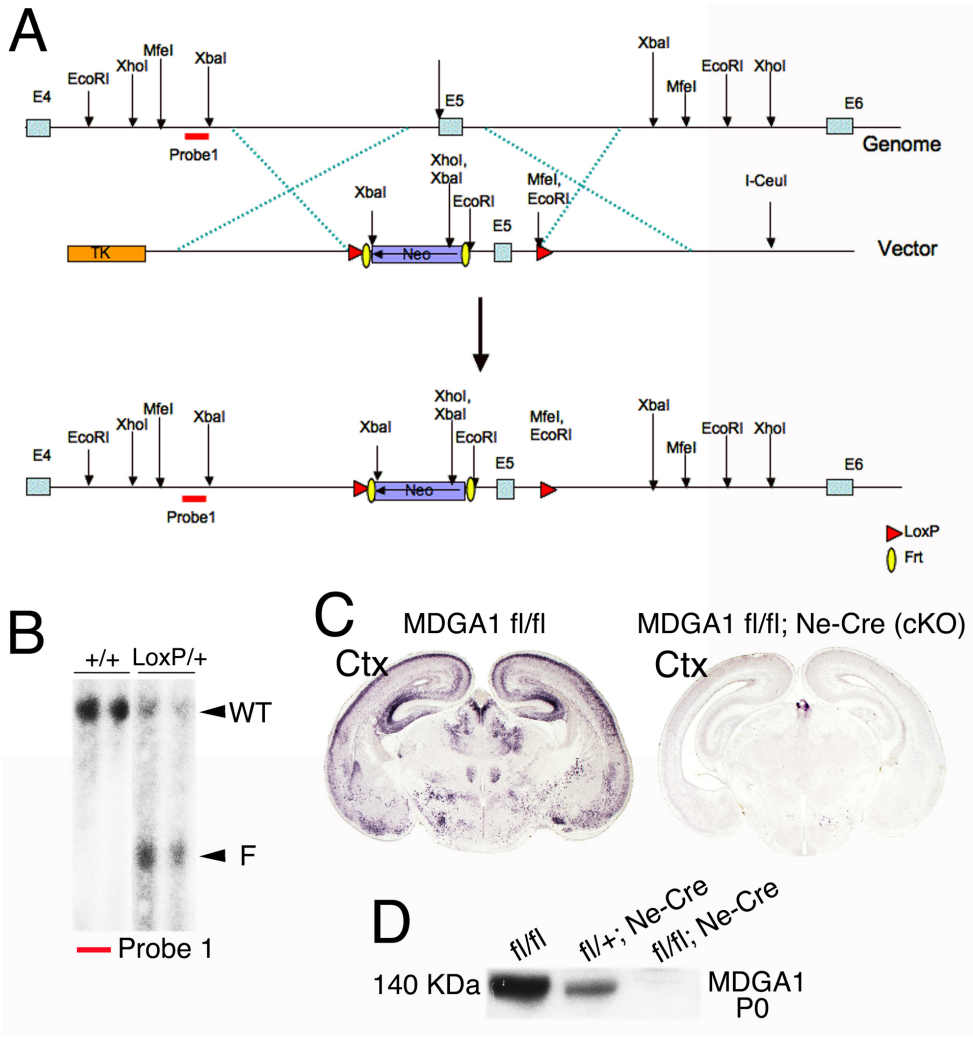

Figure S4. Generation of the conditional floxed allele for MDGA1, related to Figures 4-7. Shown are the targeting construct and strategy used to generate the MDGA1 conditional knockout mice and the effectiveness of the conditional deletion of MDGA1 using a Nestin-Cre line. A: Schematics of targeting construct and gene targeting strategy. Exon 5 of mouse MDGA1 was targeted and substituted using homologous recombination with a PGK-Neo cassette flanked by two Frt sites upstream of Exon 5. The recombined Exon 5 (MDGA1$^{fl\text{-}neo/+}$) is flanked by two LoxP sites: one site upstream of the PGK-Neo cassette and one site downstream of the recombined

Exon 5. Using a Cre/LoxP recombination strategy, we performed a conditional deletion of the MDGA1$^{fl\text{-}neo/+}$ allele. B: Successful gene targeting shown by southern blot analysis revealing the presence of the WT and LoxP bands in heterozygous mice (LoxP/+) versus control mice (+/+). C: In vivo demonstration of effective conditional deletion of the floxed MDGA1 alleles by crossing homozygous floxed MDGA1 mice (fl/fl) with a Nestin-Cre line (Ne-Cre) to generate the MDGA1 conditional knockout mice (cKO) used in this study. Shown are coronal sections of brains from P0 WT (MDGA1 fl/fl) and cKO mice (MDGA1 fl/fl;Ne-Cre) processed for MDGA1 ISH using dioxigenin-labeled riboprobes. Robust MDGA1 expression detected in the brains of P0 WT mice, including that in cortex, is not detected in the P0 cKO brain. D: Western Blot using tissue from P0 cortex of WT (fl/fl), heterozygous (fl/+; Ne-Cre) and homozygous (fl/fl; Ne-Cre) mice. The appropriate 140 KDa band revealed with MDGA1 specific antibodies is detected in both WT and heterozygous cKO mice, with a substantial reduction in the band intensity in the heterozygous mice, and is entirely absent in homozygous cKO mice. Protein levels were measured using Bradford solution and equal values of 50µg of protein were loaded in all samples. β-actin was used to normalize all samples. Abbreviations: Ctx: cortex.

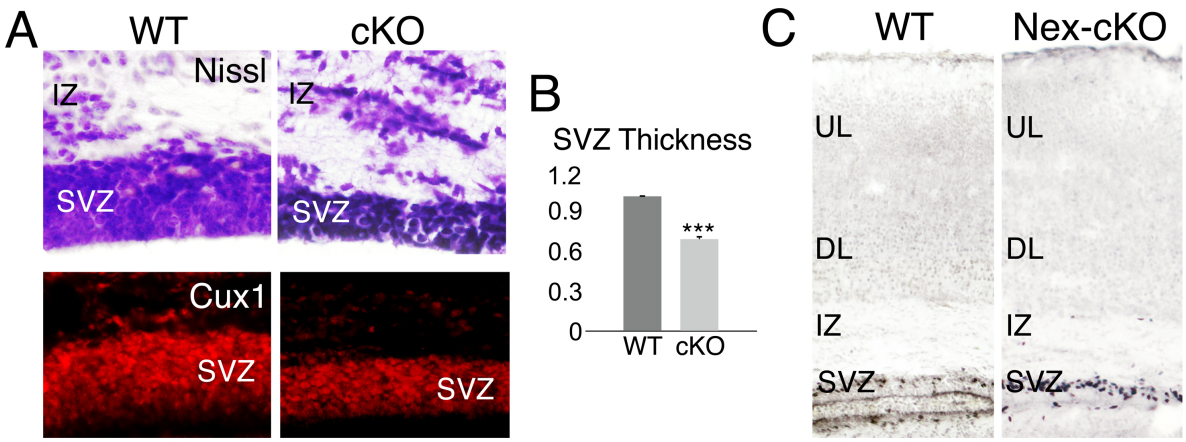

Figure S5. The reduction of thickness in the subventricular zone of the cKO persists at P0 whereas progenitors are unaffected in the Nex-cKO, related to Figures 4-5. A: Coronal sections from wild type (WT) and mice with a conditional deletion of MDGA1 using Nestin-Cre (cKO). Nissl staining and Cux1 immunolabeling demonstrate a reduction in thickness in the subventricular zone (SVZ) that is significantly reduced by 32% in the cKO compared to WT (B, 0.682±0.03, p=0.0034***, N=4). C: Shown are Tbr2 immunostained coronal sections of the neocortex from P0 WT and Nex-cKO mice created by crossing MDGA1 fl/fl mice with a Nex-Cre mouse line (Nex-cKO) that produces a conditional deletion of MDGA1 selectively from newly generated postmitotic cortical neurons. Tbr2-positive cells in both WT and Nex-Cre cortex are predominantly found in the SVZ. Ectopic Tbr2-positive cells are not detected in the Nex-Cre cortex, and the overall distribution of Tbr2-positive cells in the Nex-cKO cortex resembling that in WT cortex. Abbreviations: DL: deeper layers; IZ: intermediate zone; UL: upper layers.

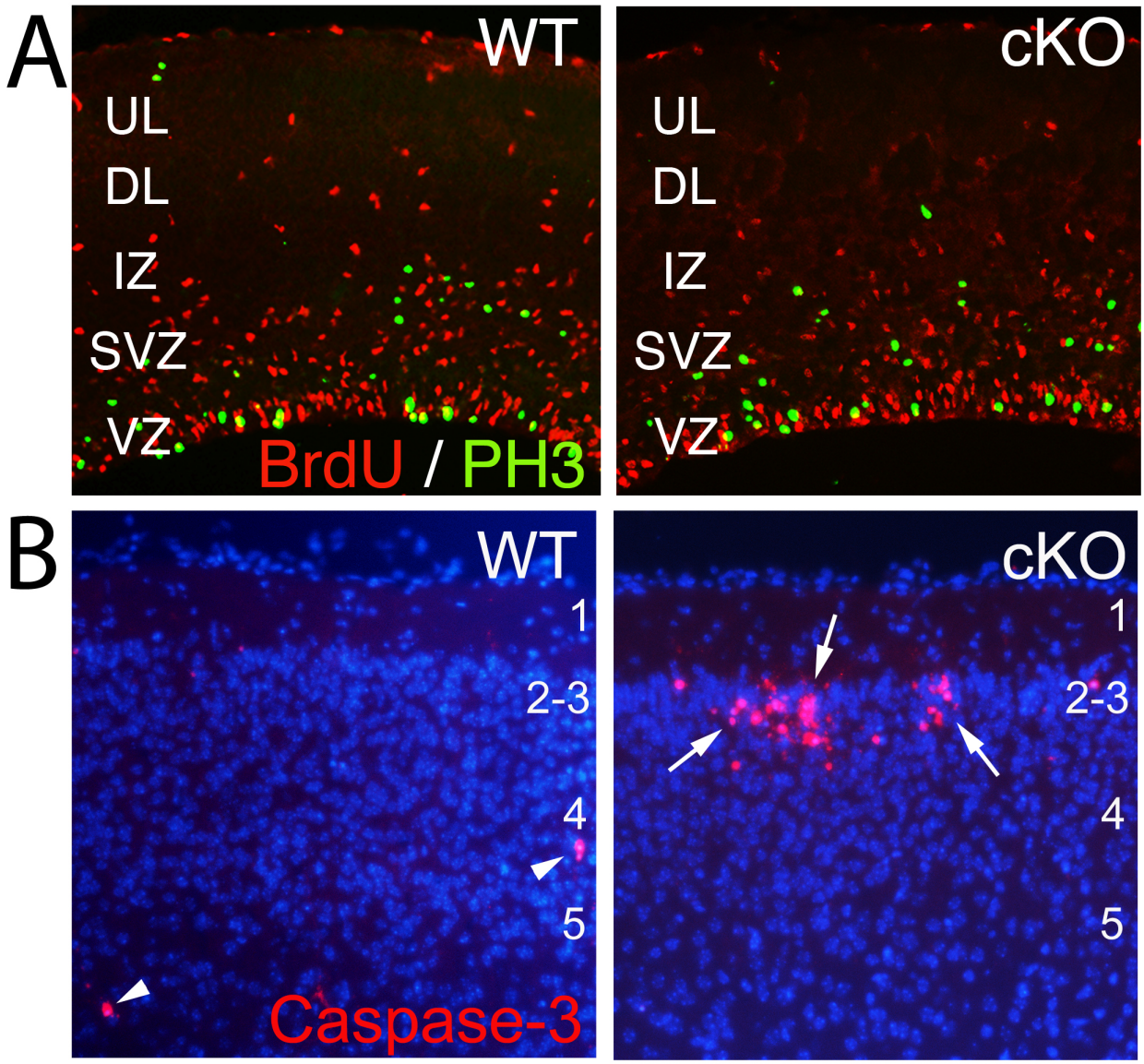

Figure S6. Ectopic Tbr2+ cells in the cortical plate of MDGA1 cKO mice are non-proliferative and most likely die by apoptosis, related to Figures 4-7. A: Shown are coronal sections of the neocortex from E16.5 wild type mice (WT) and cKO mice double immunostained for markers of cellular proliferation, BrdU (red) and Phospho-Histone3 (PH3, green), following a 2-hour pulse of BrdU. In both WT and cKO, BrdU and PH3

labeling is predominantly in the appropriate cortical proliferative zones, the ventricular zone (VZ) and the subventricular zone (SVZ). Very few cells in the upper layers (UL) or deeper layers (DL) of the cortical plate are labeled with either marker, with the overall patterns in WT and cKO closely resembling each other. This finding shows that the dense population of ectopic Tbr2-positive cells aberrantly found in the upper cortical layers of the cKO is in a non-proliferative state. B: P4 cortical sections showing Caspase-3 immunolabeling in WT and cKO. In the cKO, clusters of Caspase-3 positive cells (arrows) are observed at upper layer locations where ectopic Tbr2+ cells are found in the cKO. However, these clusters were not observed in the WT that only shows normal levels of Caspase3 positive cells deeper in the cortex (arrowheads). Abbreviations: 1-5: cortical layers 1-5; IZ: intermediate zone.

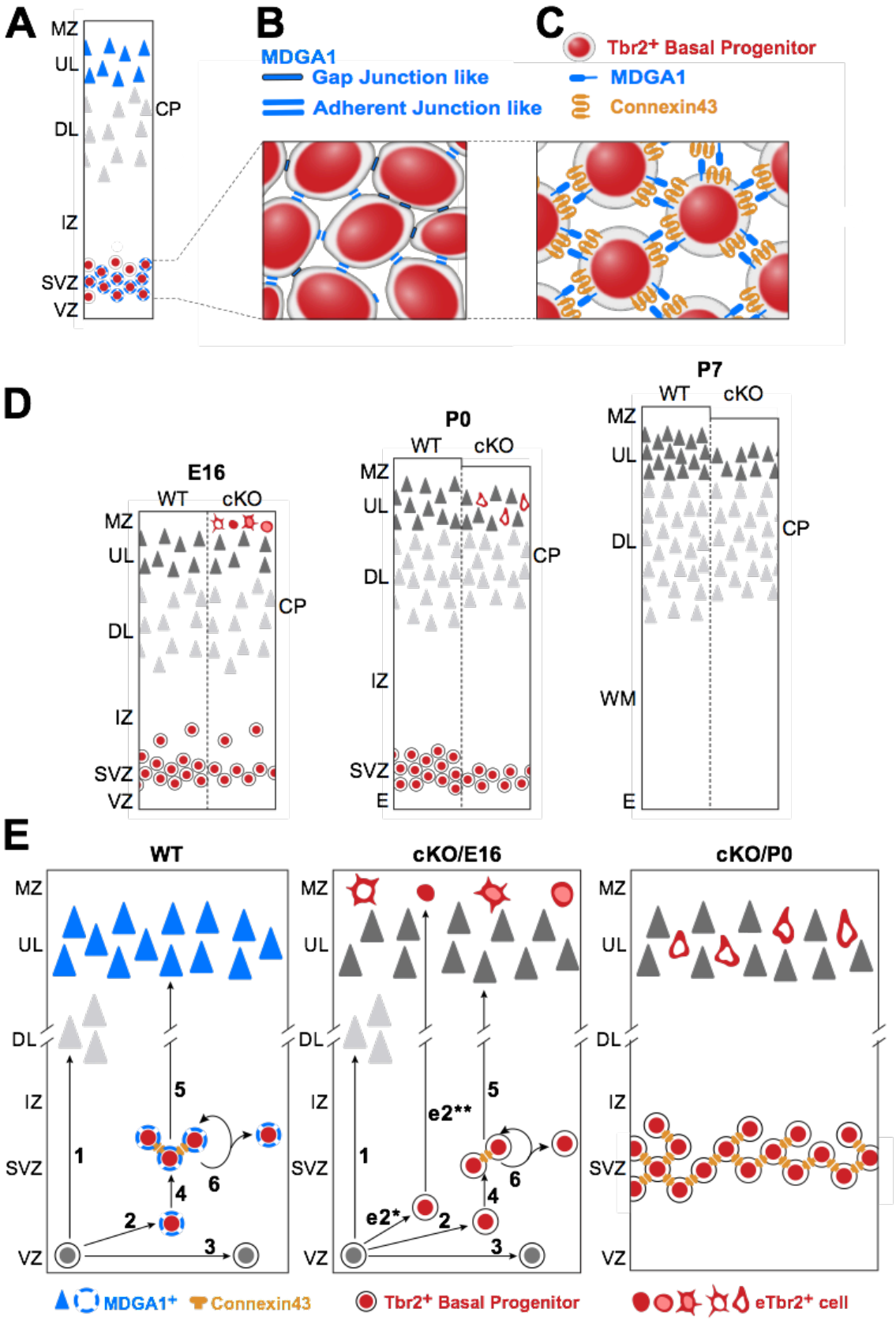
A
MZ
UL
DL
IZ
SVZ
VZ
CP
B
MDGA1
Gap Junction like
Adherent Junction like
C
Tbr2+ Basal Progenitor
MDGA1
Connexin43
D
E16
P0
P7
WT
cKO
WM
E
WT
cKO/E16
cKO/P0
e2*
e2**
MDGA1+
Connexin43
Tbr2+ Basal Progenitor
eTbr2+ cell

Figure S7. Summary of major findings from MDGA1 cKO and model for MDGA1 function in aggregation of basal progenitors to form the subventricular zone and produce cortical layer neurons, related to Figures 1-7.

A: Cell populations that express MDGA1 in the developing neocortex of mice. MDGA1 is expressed by the majority of the Tbr2+ Basal Progenitors (BPs) in the subventricular zone (SVZ, Mander's co-localization coefficient tM= 0.54±0.06) and by the upper layer (UL) neurons produced by BPs of the SVZ. MDGA1 is not expressed in deeper layers (DL).

B: MDGA1 is expressed in discrete domains of the cell membrane in apposing BPs in the SVZ. This expression pattern is found in two forms related to the separation between two apposing MDGA1+ cell membranes: one where a narrow space can be discriminated between the apposing cell membranes resembling adherent junctions; and one where the apposing cell membranes come together in a very tight association and no space is observed between them, which resembles gap junctions.

C: MDGA1 is anchored to the cell membrane of Tbr2+ BPs in the SVZ. MDGA1 co-localizes with the transmembrane gap junction protein Connexin43 (Cx43) in the cell membrane and associates with it. MDGA1 might interact in "cis" and/or in "trans" with Cx43 expressed in the same and/or adjacent BPs, respectively.

D: Conditional deletion of MDGA1 from Nestin progenitors (cKO) results in reduced proliferation and reduced number of Tbr2+ BPs in the SVZ, and an aberrant population of Tbr2+ BPs ectopically positioned at the top of the cortical plate (CP) (more details in E below). The reduced SVZ and ectopic Tbr2+ BPs are clearly evident at E16, during the peak generation of upper layer neurons by BPs of the SVZ, and later. At P0, the

ectopic Tbr2+ BPs are integrated in the upper layers of the cortical plate and have acquired a radial morphology (more details in E below) and the SVZ remains significantly reduced (E16: 0.53±0.01, p=0.0059***; P0: 0.682±0.03, p=0.0034***). In addition, at P0 and later, the width (P0: 0.830±0.02, p=0.0218**; P4: 0.781±0.05, p=0.0096***) and neuronal density (P4; 0.61±0.02, p=0.0013***) of the upper layers of the cortical plate are significantly reduced in the cKO compared to wild type (WT), with an overall reduction in neuron number to about half the WT number, due to their diminished production by the reduced SVZ. By P7, ectopic Tbr2+ cells are no longer detected. The deeper layers also present a minor reduction in thickness (P0: 0.946±0.009, p=0.01**; P4: 0.943±0.01, p=0.006***).

E: Model summarizing the function of MDGA1 in Tbr2+ BPs of the SVZ. WT: During development, radial glia of the ventricular zone (VZ) divides asymmetrically to generate deeper layer neurons (1), Tbr2+ BPs that leave the VZ and aggregate on top of it to form the SVZ (2), or to another radial glia to maintain the proliferative population in the VZ (3). The newly generated Tbr2+ BPs in the VZ express MDGA1 and Cx43 in the cell membrane. MDGA1 forms complexes with Cx43, and this interaction facilitates cell adhesion among Tbr2+ BPs to promote their aggregation in the SVZ (4). The MDGA1+/Tbr2+ BPs undergo a terminal division to generate upper layer neurons that also express MDGA1 and migrate along radial glia processes to populate the upper layers of the cortical plate (5); a small proportion of MDGA1+/Tbr2+ BPs first generate additional BPs (6). cKO: The basic scheme is similar to that in WT (2-6), except that following conditional deletion of MDGA1 from VZ progenitors, newly generated BPs in the VZ are MDGA1 deficient and a significant proportion of them fail to aggregate within

the SVZ (e2*) and instead migrate superficially to ectopic positions at the top of the cortical plate (e2**), resulting in a reduced number of BPs and reduced proliferation in the SVZ. At E16, the ectopic Tbr2+ BPs at the top of the cortical plate have a multipolar-like morphology characteristic of BPs of the SVZ but varying localization of Tbr2 protein from nuclear localization as in normal BPs of the SVZ to aberrant localization throughout the cell body. At P0, the ectopic Tbr2+ BPs are integrated in the upper layers of the cortical plate and have acquired a radial morphology resembling cortical plate neurons, with Tbr2 protein being aberrantly localized to the radial apical process and cell cytoplasm and excluded from the nucleus. They do not exhibit properties of differentiated cortical neurons nor glia, including radial glia. Abbreviations: E: ependyma; IZ: intermediate zone; MZ: marginal zone; WM: white matter.

2) SUPPLEMENTAL EXPERIMENTAL PROCEDURES

Animals

FLPe mice (Rodriguez et al., 2000) were used during production of the floxed MDGA1 mice. For staging, midday of the day of the vaginal plug was considered as E0.5 and the day of birth was termed P0. Mice were anesthetized with Avertin 2.5% (0.015 ml/gr body weight) and terminated by perfusion with cold 4% buffered paraformaldehyde (wt/vol) or Bouin's fixative. All experiments were conducted in accordance with US National Institutes of Health guidelines and were approved by the Institutional Animal Use and Care Committee of the Salk Institute.

Immunohistochemistry

For Nissl staining, 10-20 µm-thick sections were stained with 0.5% cresyl violet (wt/vol), then dehydrated through graded alcohols and mounted. For immunofluorescence, we used a FITC-conjugated goat anti-mouse (1:500, Jackson), a Cy3-conjugated goat anti-rabbit (1:500, Jackson), Alexa 488-conjugated goat anti-mouse (1:500, Molecular Probes, Invitrogen) and Alexa 594-conjugated goat anti-rabbit (1:500, Molecular Probes, Invitrogen). Sections were mounted in a medium containing DAPI (Vector) and visualized in a fluorescence microscope and/or confocal microscope. See main text for Di-Amino-Benzidine (DAB) visualization.

Electron Microscopy

90 µm thick coronal and sagittal vibratomed sections were stored in 1% paraformaldehyde and washed in 10mM Dulbecco's phosphate buffered saline (PBS) solution without calcium, magnesium, or phenol red (GE Healthcare Hyclone) and incubated in 0.3% hydrogen peroxide in PBS for 10 min, and washed thoroughly in

PBS. Any residual free aldehydes were quenched with 1% sodium borohydride in 1XPBS for 5 minutes and washed thoroughly again with PBS. Then, sections were incubated with a goat anti-MDGA1 antibody (Santa Cruz) at a 1:750 dilution in PBS containing 1% bovine serum albumin (BSA) overnight at 4°C. Then, sections were washed thoroughly with PBS containing 1% BSA and subsequently incubated with a biotinylated horse anti-goat antibody (Vector Laboratories, Inc., CA, USA) at a 1:100 dilution in PBS containing 1% BSA for two hours at RT. After several washes in PBS, sections were incubated with the Vectastain Elite ABC Kit (Vector Laboratories, Inc., CA, USA) in 0.05M Tris Buffer Saline (TBS) for 30 min at room temperature. Then several washes in PBS followed by two washes in 0.05M TBS. Immunolabeling was visualized by first incubating the tissue in 1mg/mL DAB (Thermo Scientific) in TBS for 3-5 min, followed by 1mg/mL DAB + 0.01% hydrogen peroxide. After visually confirming the reaction took place, the sections were washed in PBS several times and subsequently fixed in 1% osmium tetroxide/1.5% potassium ferrocyanide in PBS for one hour on ice, and then sections were washed three times in PBS. Finally, samples were dehydrated in a graded ethanol series (35%, 50%, 75%, 90%, 100%, 100%) and microwave infiltrated in Spurr's resin. The resin was cured at 60°C for 24 hours and the regions of interest were marked using a UV laser (355nm) from a laser capture microdissection system (Zeiss PALM MicroBeam, Jena, Germany). 70nm sections were then taken of the region of interest and imaged on a Transmission Electron Microscopy at 120kV (Zeiss Libra 120 PLUS, Oberkochen, Germany).

Proliferation Assays

Short pulses (2-hour) of BrdU (10 mg/ml) were performed by injection of 200 µl of BrdU intraperitoneally in pregnant females (E16.5). Brains from BrdU injected mice were dissected and prepared for paraffin sections. Co-labeling experiments were performed using a rat anti-BrdU (Abcam) and a rabbit anti-PH3 (Millipore).

Cell Counting and Statistics

All analyses were done blind to genotype. An equal number (N) of WT and cKO mice were used for the statistical analyses. For every counting experiment, similar coronal or sagittal levels were used in both WT and cKO, and cell counting was performed using the same grid area at matching anatomical positions. For every sample, three consecutive positions in the same area were measured to calculate an average per sample. Measurements and cell counting were performed using plugins from the FIJI software (NIH, http://rsb.info.nih.gov/ij/) and analyzed using Numbers software. The Mander's co-localization coefficient (tM) using the thresholding algorithm of Costes (Costes et al., 2004, Mander, 1993, Sanchez-Alcaniz et al., 2011, Mazumder et al., 2014, Filadi et al., 2015) was calculated in an N=13 by measuring the region of interest (ROI) in similar sections throughout samples. The tM (means±SEM) ranges from 0 to 1, where 0 is no correlation and 1 is perfect overlap. We used the coloc2 analysis plugin from the FIJI software (NIH, http://rsb.info.nih.gov/ij/) to determine the tM. Statistical significance was determined using un-paired two-tailed t test, P values < 0.05 (*) were considered statistically significant.

Cell Culture

293 cells were plated and grown in medium containing DMEM, 10% FBS and antibiotics (1x PS) at 37°C in an incubator at 5% CO2. The day of the transfection cells were at 70-

80% confluence. Transfection was done using the PolyFect Transfection Reagent (Qiagen). We co-transfected using either full length MDGA1 (Litwack et al., 2004) or Myc-tagged full length MDGA1 (Myc-His tagged MDGA1)(Litwack et al., 2004) together with a GFP plasmid to confirm the effectiveness of the transfection. Immunocytology was done as previously described (Sahara and O'Leary, 2009). Briefly, cells were washed in PBS and fixed in 4% PFA for 30 minutes. Then, after washes and permeabilization steps, cells were incubated with the correspondent primary antibodies: rabbit anti-MDGA1 or mouse anti-Myc. For co-localization, we used a rabbit anti-Connexin43. DAPI was used for counterstaining.

Biochemistry: Enrichment Differential Centrifugation, Immunoprecipitation and PI-PLC assay

Enrichment Differential Centrifugation Assay

We isolated P7 WT cortices and separated a SVZ/VZ fraction and a CP fraction and homogenized them to break cell membranes and mix cellular components. Pellet and supernatant were separated and the supernatant was processed through an increase of graded centrifugation steps from 600g to 100.000g; removing the pellet in every step and proceeding with the supernatant (Elortza et al., 2003, Schindler and Nothwang, 2009b, Schindler and Nothwang, 2009a, Lingwood and Simons, 2007). In the final centrifugation done at 100,000g, two main fractions were obtained: soluble and microsome. Those fractions were resolved by SDS/PAGE and the immunoblot was incubated with rabbit anti-MDGA1 antibodies and developed by a chemiluminescence assay (Amersham Pharmacia, Roche).

Immunoprecipitation (IP)

WT cortex (E18, P7) and 293 cells transfected with Myc-MDGA1 were collected and processed for protein extraction. The concentration of protein was measure using Bradford's assay. A standard IP protocol was used as described (Lim et al., 2008). Briefly, after a pre-clear step, protein-G sepharose beads (GE Healthcare, Invitrogen) were incubated overnight at 4°C and in rotation with the protein sample and the IP antibody: either mouse anti-Myc, rabbit anti-Connexin43 or rabbit anti-MDGA1. As a negative control we transfected cells with Myc-NFkB (Myc-His tagged Nuclear Factor Kappa light chain B cell enhancer binding protein) (Sen and Baltimore, 1986). Samples were washed and re-suspended in standard Western Blot sample buffer. After boiling the IPs and whole cell extracts (positive controls), samples were resolved in SDS/PAGE and subjected to immunoblot analysis using an antibody against the potentially associated protein that co-IPs: rabbit anti-Connexin43 or rabbit anti-MDGA1. Blots were developed using standard chemiluminescence assays (Amersham Pharmacia, Roche).

Phosphatidylinositol-Specific Phospholipase C Assay (PI-PLC)

PI-PLC assay was done essentially as previously described (Litwack et al., 2004). Briefly, P0 and adult WT mouse cortices were isolated, homogenized, and the crude extract was incubated overnight with the Bacillus cereus PI-PLC (Molecular Probes, Invitrogen) at a concentration of 0.25 U PI-PLC at 37°C. As a control we processed a sample under the same conditions but without the PI-PLC. Samples were then processed for SDS/PAGE and immunoblotted using a rabbit anti-MDGA1 antibody. Blots were developed by chemiluminescence (Amersham Pharmacia, Roche).

Gene targeting and generation of floxed MDGA1 mice

We targeted Exon5, which is the first coding exon of MDGA1, using a targeting vector that by homologous recombination replaced endogenous Exon5 for a PGK-Neo cassette containing a Neomycin-resistance gene flanked by two Frt sites upstream of Exon5. Two LoxP sites were also located upstream of the first Frt site and downstream of the recombined Exon5 (MDGA1$^{fl\text{-}neo/+}$) for Cre/LoxP recombination.
Floxed MDGA1 (MDGA1^{fl}) ES cell clones were obtained by electroporation of the targeting vector (MDGA1$^{fl\text{-}neo/+}$) into ES cells. Those ES cells were screened by southern blot using specific 5' and 3' probes. Three positive clones carrying the MDGA1$^{fl\text{-}neo/+}$ cassette were selected, injected into C57BL/6J blastocysts and the resulting chimeras were mated to C57BL/6J females to obtain germ-line transmission. Heterozygous mice MDGA1$^{fl\text{-}neo/+}$ were mated with FLPe mice (Rodriguez et al., 2000) to remove the Neo cassette. MDGA1$^{fl/fl}$ mice were obtained by crossing heterozygous (MDGA1$^{fl/+}$) mice.

For genotyping, we use the following primers: for *Flox* forward 5'-AAGCACTGGCCGTGAAGAT-3' and reverse 5'-GGGTCTCCTGAGCTCACTGT-3' and for *Cre*: forward 5'-GTGTTGCCGCGCCATCTGC-3' and reverse 5'-CACCATTGCCCCTGTTTCACTATC-3'. To confirm that the excision and the system worked, we extract DNA from mice tails (crossed with Nestin-Cre) and performed PCR by using external primers: forward 5'-GGAAGCAAGGAAATTGGACA-3' and reverse 5'-GGGTCTCCTGAGCTCACTGT-3'.

MDGA1$^{fl/fl}$ mice were mated with Nestin-Cre mice and Nex-Cre mice. Double heterozygous for MDGA1$^{fl/+}$;Nestin-Cre (cKO) and MDGA1$^{fl/+}$;Nex-Cre (Nex-cKO) were viable and fertile. Double homozygous for MDGA1$^{fl/fl}$; Nex-Cre were viable and fertile,

whereas MDGA1$^{fl/fl}$; Nestin-Cre did not follow Mendelian ratio suggesting some embryonic lethality.

3) SUPPLEMENTAL REFERENCES

COSTES, S. V., DAELEMANS, D., CHO, E. H., DOBBIN, Z., PAVLAKIS, G. & LOCKETT, S. 2004. Automatic and quantitative measurement of protein-protein colocalization in live cells. *Biophys J,* 86**,** 3993-4003.

ELORTZA, F., NUHSE, T. S., FOSTER, L. J., STENSBALLE, A., PECK, S. C. & JENSEN, O. N. 2003. Proteomic analysis of glycosylphosphatidylinositol-anchored membrane proteins. *Mol Cell Proteomics,* 2**,** 1261-70.

FILADI, R., GREOTTI, E., TURACCHIO, G., LUINI, A., POZZAN, T. & PIZZO, P. 2015. Mitofusin 2 ablation increases endoplasmic reticulum-mitochondria coupling. *Proc Natl Acad Sci U S A,* 112**,** E2174-81.

LIM, Y. S., MCLAUGHLIN, T., SUNG, T. C., SANTIAGO, A., LEE, K. F. & O'LEARY, D. D. 2008. p75(NTR) mediates ephrin-A reverse signaling required for axon repulsion and mapping. *Neuron,* 59**,** 746-58.

LINGWOOD, D. & SIMONS, K. 2007. Detergent resistance as a tool in membrane research. *Nat Protoc,* 2**,** 2159-65.

LITWACK, E. D., BABEY, R., BUSER, R., GESEMANN, M. & O'LEARY, D. D. 2004. Identification and characterization of two novel brain-derived immunoglobulin superfamily members with a unique structural organization. *Mol Cell Neurosci,* 25**,** 263-74.

MANDER, E. E. M., VERBEEK, F.J., ATEN, J.A. 1993. Measurement of co-localization of objects in dual-color confocal images. *Journal of Microscopy,* 169**,** 375-382.

MAZUMDER, P., PRAJAPATI, S., LOKAPPA, S. B., GALLON, V. & MORADIAN-OLDAK, J. 2014. Analysis of co-assembly and co-localization of ameloblastin and amelogenin. *Front Physiol,* 5**,** 274.

RODRIGUEZ, C. I., BUCHHOLZ, F., GALLOWAY, J., SEQUERRA, R., KASPER, J., AYALA, R., STEWART, A. F. & DYMECKI, S. M. 2000. High-efficiency deleter mice show that FLPe is an alternative to Cre-loxP. *Nat Genet,* 25**,** 139-40.

SAHARA, S. & O'LEARY, D. D. 2009. Fgf10 regulates transition period of cortical stem cell differentiation to radial glia controlling generation of neurons and basal progenitors. *Neuron,* 63**,** 48-62.

SANCHEZ-ALCANIZ, J. A., HAEGE, S., MUELLER, W., PLA, R., MACKAY, F., SCHULZ, S., LOPEZ-BENDITO, G., STUMM, R. & MARIN, O. 2011. Cxcr7 controls neuronal migration by regulating chemokine responsiveness. *Neuron,* 69**,** 77-90.

SCHINDLER, J. & NOTHWANG, H. G. 2009a. Enrichment of brain plasma membranes by affinity two-phase partitioning. *Methods Mol Biol,* 528**,** 119-26.

SCHINDLER, J. & NOTHWANG, H. G. 2009b. Isolation of plasma membranes from the nervous system by countercurrent distribution in aqueous polymer two-phase systems. *Methods Mol Biol,* 564**,** 335-40.

SEN, R. & BALTIMORE, D. 1986. Multiple nuclear factors interact with the immunoglobulin enhancer sequences. *Cell,* 46**,** 705-716.